A BIM-based Method for Estimating Radiation Source Strengths Using Field-measured Dose Rates

Hyong Chol Kim*, Jae Hee Roh, Moonjoo Gil, Young Jin Lee
NSE Technology Inc., 5F Convergence Technology Research Commercialization Center
218 Gajeong-ro, Yuseong-gu, Daejeon, 34129, Korea
**Corresponding author: hckim@nsetec.com*

***Keywords:** source strength, dose rate, measurement, BIM, nuclear power plant, decommissioning

1. Introduction

Radiological characterization is performed to obtain information on the amount, type, and distribution of radionuclides for decommissioning of a nuclear power plant. The results of the characterization can be used to confirm the decommissioning process concerning approaches, resources, cost evaluations of activities, and the appropriateness of timelines.

In general, radioactive contamination of a component is determined through direct measurement or sampling and analysis of the component of interest. However, it is known that dose rate measurements of radiation fields can provide an acceptable estimate of the activity if the relationship between activity content and radiation field is well established [1]. Then, it would be beneficial if the activities of radiation sources can be determined using this approach without incurring substantial effort and cost for sampling and laboratory analysis.

Recently, 3D modeling is commonly used to visualize the decommissioning process of nuclear facilities, and the radiological and material/component data are processed with reference to the 3D model [2], and BIM (Building Information Modeling)-based frameworks are often used to manage the decommissioning process [3]. Once a BIM is built for a nuclear facility, its 3D model can be used to establish the physical relationship between the radioactive sources and the radiation field.

Previously, the authors have reported software that implemented a 3D model-based method for determining activities of radiation sources using the dose rates measured in the field, and referred to the software as BIMRAD [4]. The present study focuses on demonstrating the applicability of BIMRAD in situations that may be encountered at the decommissioning scenes of a nuclear power plant where multiple components are deployed.

2. Methods

2.1 Solution of Source Strength from Measured Dose Rates

The dose rate response term (R_{mj}) at position r_m due to a source at position r_j of unit activity strength in Bq/cm^3 with volume V_j can be expressed as a function of the distance between the source and the measurement point and the path length (T) through the medium, using the point kernel method [4]. This function also includes several other variables such as the gamma energy of the source, the flux-to-dose-rate conversion factor, the attenuation coefficient, and the buildup factor of the medium.

Denoting the source strength of source j as S_j, the dose rate (D_m) measured at position m can be expressed as the sum of contributions from all sources as follows:

$$D_m = \sum_{j=0}^{N}\left[R_{mj}\cdot S_j\right] \ (m = 1,\cdots,M; M \geq N)\,, \qquad (1)$$

where M is the number of measured points and N is the number of sources. Here, M is assumed to be greater than or equal to N.

The set of inverse problem equations for S_j that satisfy Eq. (1) with least square error can be obtain as follows:

$$\sum_{j=1}^{N}[(\sum_{m=1}^{M} R_{mk}R_{mj})\cdot S_j] = \sum_{m=1}^{M}[D_m R_{mk}] \quad (\mathrm{k}=1,\cdots,N)\,. \qquad (2)$$

The source strength S_j can then be obtained by solving Eq. (2) with non-negative condition of $S_j \geq 0$. The activity (A_j) of source j is calculated by $A_j = S_j V_j$.

Now that the source strength solution has been obtained, the dose rates can be evaluated at any designated position by substituting the source strengths into Eq. (1).

2.2 Extraction of Geometric Parameters and Material Properties

Radiation sources and shielding objects are represented by solid STL models in the 3D space of BIMRAD.

In BIMRAD, the path length T is determined by finding pairs of coordinate points on the inlet and outlet surface meshes of the shielding objects at which the line from the source to the measurement point intersects. For mathematical convenience, a source object is represented as a phantom of an equivalent volume of a simple geometric shape such as a sphere, a cylinder, a pipe, or a cuboid. Phantoms can be subdivided into multiple cells to better approximate large volume sources. The self-shielding length of the source is determined algebraically by finding the intersection of the line connecting to the

measurement point from the center of each cell with the surface equation describing the outer surface of the phantom.

The data library for attenuation coefficients and buildup factors was built using ANSI/ANS 6.4.3-1991, and the dose rate conversion factors were taken from ICRP-51. Nuclide data of gamma energies and branching ratios were obtained from IAEA's Live Chart of Nuclides [5]. The material properties of the objects in 3D space were linked using a typical data management scheme.

3. Simulated Experiments

3.1 3D Test Scene

In order to evaluate the predictive performance of BIMRAD in the decommissioning site, a test scene of about 100 m^2 was configured by placing several objects. Fig. 1 shows the planar layout of the test radiation scene displayed on a grid with a scale size of 1m.

The upright columns were placed to simulate cylindrical steel beams with a diameter of 20 cm and a height of 1m. As shown in the figure, they were arranged in a row at 2 m intervals in the x-direction. A pipe object having an inner diameter of 10 cm, an outer diameter of 20 cm, and a length of 2 m was placed horizontally on the top level of the columns. The columns and the pipe were provided as potential sources, and were labeled S-1 through S-6 as shown in the figure. In addition, a shielding wall of lead having a thickness of 20 cm and a width of 5 m was placed in the right area to provide partial shielding. Ten measurement points were set on a plane at a height of 0.5 m and were labeled with their respective numbers.

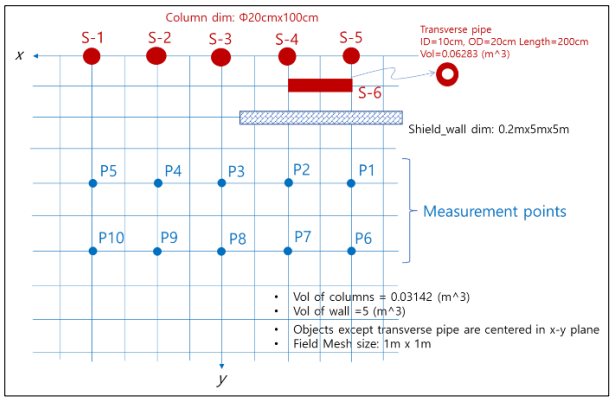

Fig. 1. Planar layout of the reference radiation scene.

Fig. 2 shows the 3D image of the above test scene generated by BIMRAD, where the radiation sources are shown in red, the shield wall is shown in dark green, and the measurement points are shown as yellow dots.

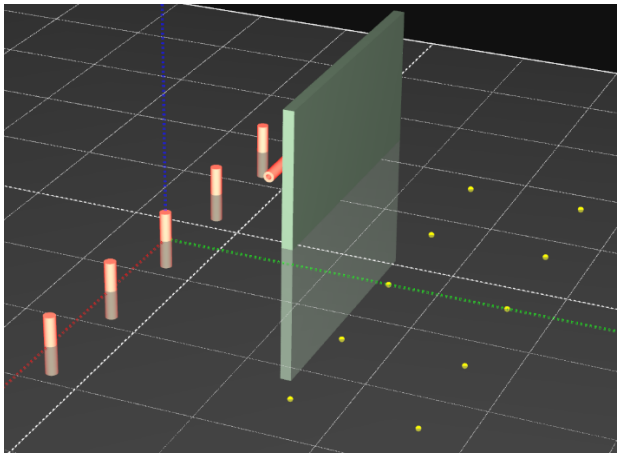
Fig. 2. 3D image of the test scene with the measurement points displayed on an imaginary plane.

3.2 Dose Rates at Measurement Points and Source Strength Estimation

Dose rates at the measurement points were determined by MCNP. The MCNP calculations were performed separately for each source. When there are multiple sources in a scene, due to the additive nature of the radiation, the dose rates can be determined by a weighted sum of source contributions.

Table I shows the dose rates evaluated in $\mu Sv/hr$ at the 10 measurement points shown in Fig. 1 for the given source strengths shown in Table II below. Table I also shows the dose rate contribution of each source.

Table I: Dose rates at the measurement points.

Meas. Points		**P1**	**P2**	**P3**	**P4**	**P5**
Contri-butions by sources	S-1	62.7	98.3	159.8	255.6	320.0
	S-2	9.34	405.9	643.5	801.0	640
	S-3	15.84	43.1	491.4	386.1	239.5
	S-4	162.2	259.4	144.9	812.0	492.3
	S-5	519.4	326.1	107.9	39.8	628.7
	S-6	1304.1	1304.6	342.5	81.2	320.1
Dose rates ($\mu Sv/hr$)		2073.6	2437.4	1889.9	2375.7	2640.6
Meas. Points		**P6**	**P7**	**P8**	**P9**	**P10**
Contri--butions by sources	S-1	50.3	70.4	97.7	127.2	141.5
	S-2	176.8	246.6	319.1	354.4	318.3
	S-3	13.6	21.6	217.4	192.8	147.1
	S-4	89.1	110.4	84.0	45.9	356.9
	S-5	220.3	178.9	99.3	47.0	24.7
	S-6	556.9	556.9	300.1	118.2	49.6
Dose rates ($\mu Sv/hr$)		1106.8	1184.8	1117.7	885.4	1038.1

The sources were assumed to be Co-60 steel and the strengths were arbitrarily assigned in the LLW (low-level waste) range, but they were set to roughly balance the contributions between the shielded and unshielded sources. The column sources were depicted as cylindrical phantoms with 2x4x5 cells in the (r,θ,l) direction, and the pipe source was depicted as a pipe phantom with 1x4x5 cells.

Table II shows the source strength results estimated by BIMRAD using the dose rates shown in Table I against the given source strength in MBq/cm^3. As shown in the table, the estimation error is within $\pm$40%, which is

comparable to the 50% uncertainty established in similar applications [6].

Table II: Estimation results of the source strengths.

Sources	S-1	S-2	S-3	S-4	S-5	S-6
Given	2	5	3	10	20	20
Estimated	2.05	5.89	3.53	12.19	27.65	18.04
Error (%)	+2.6	+17.7	+17.6	+21.9	+38.3	-9.8

3.3 Radiation Field Reconstruction

Once the source strengths are determined, the radiation contours of the field can be generated using Eq. (1). Whereas dose rates were measured at only a few designated locations, now they are available for all locations. Fig. 3 shows the radiation contours of the test scene generated by BIMRAD. It can be seen that the radiation contours are well delineated as expected for the placement of the source and shield.

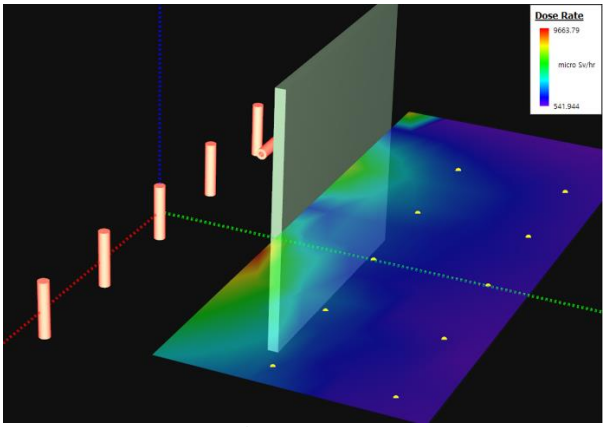

Fig. 3. Radiation contours of the test scene generated by BIMRAD.

To confirm the consistency of the proposed method, the dose rates were re-calculated by BIMRAD at the measurement points and compared to the measured values in Table II. The re-calculated dose rates were within ±20% of the measured values.

Table II: Re-calculated dose rates compared to the measured

Meas. Points	P1	P2	P3	P4	P5
Measured ($\mu Sv/hr$)	2073.	2437.	1889.	2375.	2640.
Re-calculated ($\mu Sv/hr$)	1702.	2336.	2051.	2422.	2707.
Error (%)	-17.9	-4.1	+8.5	+1.9	+2.5
Meas. Points	P6	P7	P8	P9	P10
Measured ($\mu Sv/hr$)	1106.	1184.	1117.	885.4	1038.
Re-calculated ($\mu Sv/hr$)	1057.	1215.	1213.	934.7	1043.
Error (%)	-4.5	+2.6	+8.5	+5.6	+0.43

The errors of the re-calculated dose rates are much lower than those of the source strengths. This is because the uncertainties associated with the radiation attenuations in the media are cancelled out in the source-to-receptor and receptor-to-source paths. As a result, the exposure estimation in the field is more accurate than the source activity estimation.

Fig 4. shows an image of a radiation work path drawn on the scene and the results of exposure to the work.

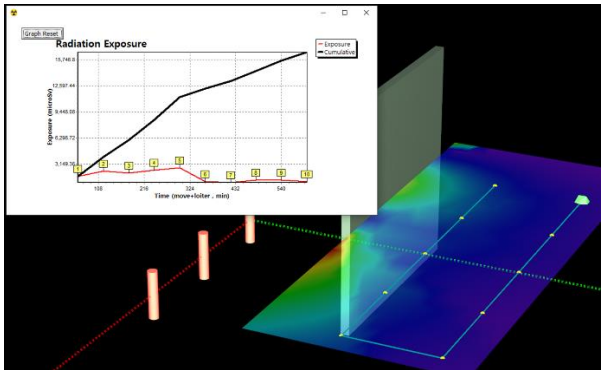

Fig. 4. A radiation work path and the associated radiation exposure graph.

3.4 Source Identification

In actual surveying area, the site technicians' knowledge is utilized for locating sources or hotspots [7]. However, there may be cases where the sources are not exactly known. Suppose the object S-4 is not a radiation source, so the source strength of S-4 is 0. In this case, the dose rates evaluated by MCNP change as shown in Table III.

Table III: Dose rates when S-4 is not a source.

Meas. Points	P1	P2	P3	P4	P5
Dose rates ($\mu Sv/hr$)	1911.4	2178.0	1745.1	1563.7	2148.3
Meas. Points	P6	P7	P8	P9	P10
Dose rates ($\mu Sv/hr$)	1017.7	1074.4	1033.6	839.5	681.2

Table IV shows the source strength results estimated by BIMRAD using the dose rates of Table III compared to the changed given source strengths. As shown in Table IV, the estimation errors were also within about ±40%. It is noted that source strength of S-4 was correctly estimated as 0. Therefore, when the sources are not known exactly, if all possible target objects are set as sources in BIMRAD, then the source strength estimation can tell which objects are the real sources.

Table IV: Results of the source strength estimation for the case of Table III.

Sources	S-1	S-2	S-3	S-4	S-5	S-6
Given	2	5	3	0	20	20
Estimated	1.84	6.25	3.55	0	28.0	18.4
Error (%)	-7.9	+25.0	+18.4	0	+40.1	-7.8

4. Conclusions

A BIM-based method for estimating radiation source strengths using the field-measured dose rates has been proposed and tested in a test scene simulating a radiation work area that can be encountered in plant decommissioning. The proposed method has been successfully shown to provide reasonable estimates of the source strengths when the measured dose rates are provided for the scene.

The source strength in MBq/cm^3 thus obtained can be easily converted into the activity concentration in *Bq/g*

that is commonly used in the plant decommissioning management to classify the radioactive wastes.

The estimation accuracy for source strength was comparable to that in similar applications. While it is preferable to accurately designate source objects in BIM, if all potential target objects are set as sources in the BIM, the non-source objects can be found by the estimation results of the source strengths.

When the dose rates were re-calculated on the measurement points using the estimated source strengths, the dose rates were reproduced with a reasonable accuracy. Therefore, once an estimate of the source strengths is obtained, dose rates can be easily calculated even for unmeasured points and used for the radiation exposure evaluation for a planned radiation work at the site.

An accurate estimate of the radioactive inventory of a nuclear facility is essential for proper planning and safe decommissioning. This study proposes a method for assessing the radionuclide inventory due to contamination without the need of sampling and laboratory analysis. While the accuracy of the method is expected to vary depending on the geometrical complexity of the scene and the quality of the measurement data, the proposed method should be a valuable tool for inventory estimation and exposure analysis in decontamination or decommissioning operations.

ACKNOWLEDGEMENTS

This work was supported by the Korea Institute of Energy Technology Evaluation and Planning (KETEP) and the Ministry of Trade, Industry and Energy (MOTIE) of the Republic of Korea (Nos. 20217910100130 and 20191510301290).

REFERENCES

[1] Radiological Characterization of Shut Down Nuclear Reactors for Decommissioning Purposes, Technical Reports Series No. 389, International Atomic Energy Agency, 1998.
[2] Managing the Unexpected in Decommissioning, IAEA Nuclear Energy Series No. NW-T-2.8, International Atomic Energy Agency, 2016.
[3] A. H. Oti, et al., A BIM-driven framework for integrating rules and regulations in the decommissioning of nuclear power plants, Construction Innovation, 22 (4), pp. 809-830, 2022.
[4] H. C. Kim, et al., A 3D Model-based Estimation Method of Radiation Source Activity from Dose Rates Measured in the Field, Transactions of the Korean Nuclear Society Spring Meeting, Jeju, Korea, May 18-19, 2023.
[5] Live Chart of Nuclides, https://www-nds.iaea.org/relnsd/vcharthtml/VChartHTML.html.
[6] H. Toubon, et al., Use of Mathematical Modeling in Nuclear Measurements Projects, 2011 Proceeding 2nd International Conference on Advancements in Nuclear Instrumentation, Measurement Methods and their Applications, Ghent, Belgium, 6-9 June, 2011.
[7] P. Tran, Demonstration of Advanced 3D ALARA Planning Prototypes for Dose Reduction, No. 1025310, Electric Power Research Institute, 2012.